

Kinetics of the Unimolecular Decomposition of iso-C₃H₇: Weak Collision Effects in Helium, Argon, and Nitrogen

P. W. Seakins,[†] S. H. Robertson,[‡] and M. J. Pilling^{*†}

Physical Chemistry Laboratory, South Parks Road, Oxford, OX1 3QZ, UK

I. R. Slagle, G. W. Gmurczyk,[§] Á. Bencsura,[⊥] and D. Gutman^{*}

Department of Chemistry, Catholic University of America, Washington, D.C. 20064

W. Tsang^{*}

Chemical Kinetics Division, National Institute of Standards and Technology, Gaithersburg, Maryland 20899

Received: October 26, 1992

Rate constants for the unimolecular decomposition of iso-C₃H₇ have been determined by laser flash photolysis coupled with photoionization mass spectrometry, over the temperature range 720–910 K. The reaction was studied in He, at densities of (3–30) × 10¹⁶ atoms cm⁻³. More limited measurements were made for Ar and N₂. The reaction is in the falloff region under all conditions studied. Three methods of data analysis were employed: (i) A transition state model was constructed by reference to literature values of dissociation and association limiting high-pressure rate constants over the temperature range 177–910 K. The model gives $k_1^\infty = 6.51 \times 10^7 T^{1.83} \exp(-17793/T) \text{ s}^{-1}$ and $k_1^\infty = 9.47 \times 10^{-15} T^{1.16} \exp(-440/T) \text{ cm}^3 \text{ molecule}^{-1} \text{ s}^{-1}$ for dissociation and association, respectively. The model was incorporated into a modified strong collision model and the data fitted using $\langle \Delta E \rangle_{\text{down}}$ as a variable parameter, giving 136 cm⁻¹ (He), 130 cm⁻¹ (Ar) and 129 cm⁻¹ (N₂). (ii) A Troe analysis, using the transition-state model to determine both k_1^∞ with S_T and employing k_1^0 as the variable parameter, is consistent with $\langle \Delta E \rangle_{\text{down}} = 200 \text{ cm}^{-1}$ for He. (iii) Finally, the microcanonical rate constants for dissociation were calculated by inverse Laplace transformation of the association rate constants of Harris and Pitts and incorporated in a master equation analysis with $\langle \Delta E \rangle_{\text{down}}$ and ΔH_0^0 as the variable parameters. The analysis gives $\langle \Delta E \rangle_{\text{down}} = 210 \text{ cm}^{-1}$ for He and $\Delta H_{f,298}^0$ (iso-C₃H₇) = 21.0 kcal mol⁻¹.

I. Introduction

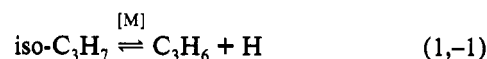
The unimolecular decomposition of alkyl radicals is an important aspect of the chemical kinetics of many high-temperature processes including the pyrolysis and oxidation of hydrocarbons.^{1–3} To date, information on the rate constants of these reactions is derived largely from indirect studies based on product analyses of complex kinetic systems in which the decomposition reaction of interest is an important elementary step.^{4–10} These studies, typically conducted at pressures of several hundred Torr, have provided rate constants near the high-pressure limit and at temperatures between 600 and 800 K. Rate coefficients at or near room temperature and indications of falloff behavior of these reactions (i.e., measures of the collisional energy-transfer parameters) are available from investigations of the reverse addition reactions conducted at lower pressures.^{11–16}

The magnitude and temperature dependence of the parameters such as $\langle \Delta E \rangle_{\text{down}}$ (the average energy transferred in a deactivating collision) required to predict the falloff behavior of these unimolecular reactions at elevated temperatures are largely uncertain for reactions involving polyatomic free radicals, although very recent investigations have provided some information on this subject for the C₂H₅^{17,18} and CH₃CO¹⁹ radicals. In the case of closed-shell hydrocarbon molecules, information is available which has been correlated.²⁰ High-temperature unimolecular decomposition data in the temperature range 1200–2500 K (using

argon as the bath gas) can be fitted using step sizes down per collision of the order of 400–800 cm⁻¹. Near room temperature, values in the 100-cm⁻¹ range are required to fit pressure-dependent rate coefficients for the reverse combination process.

The study of the decomposition of simple alkyl radicals provides an opportunity to characterize energy transfer of hydrocarbon species at temperatures intermediate between those of the investigations of addition reactions conducted near ambient temperature and the shock tube studies of hydrocarbon dissociations. These free-radical decompositions involve species with much lower levels of excitation, typically between 20–40 kcal mol⁻¹ (versus 80–105 kcal mol⁻¹ for stable hydrocarbon molecules), and hence are processes most conveniently studied at intermediate temperatures, 500–1000 K.

In this paper we present the results of an investigation of the unimolecular decomposition of the isopropyl radical:



using three bath gases: helium, argon, and nitrogen. Unimolecular rate coefficients, $k_1(T, M)$, were measured as a function of temperature (typically 750–900 K) and density ((3–30) × 10¹⁶ atoms cm⁻³ in the case of He). The experiments have provided significant sections of isothermal unimolecular falloff curves (k_1 vs [M]) at 14 different temperatures plus more limited measurements at three others (in the case of M = He).

Many pressure dependent reactions play important roles in processes occurring outside of the conditions that can be conveniently measured in the laboratory. Extrapolation of laboratory data, based on sound theoretical models, is the best way to gauge the contribution of any particular elementary reaction under these conditions. In addition, theoretical models

[†] Present address: School of Chemistry, University of Leeds, Leeds, LS2 9JT, UK.

[‡] Present address: Department of Chemistry, University of Cambridge, Cambridge, CB2 1EW, UK.

[§] Present address: Warsaw University of Technology, Institute of Heat Engineering, 00-665 Warszawa, Poland.

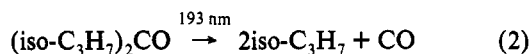
[⊥] On the leave from the Central Research Institute for Chemistry, Hungarian Academy of Sciences, H-1525, P.O. Box 17, Budapest, Hungary.

provide some insight into the nature of both inter- and intramolecular energy transfer and hence validation of such models is of great importance. In this investigation we have applied three theoretical methods, modified strong collision/RRKM (MSC/RRKM), Troe modified Lindemann–Hinshelwood, and inverse Laplace transform/master equation (ILT/ME) techniques to model the observed weak collision effects in this unimolecular reaction. A discussion of the results obtained with the three methods and the physical bases of MSC/RRKM and ILT/ME methods are included.

Limitations in the experimental conditions made it impossible to reach the high pressure limit. Fortunately, the high-pressure-limit rate coefficient, k_1^∞ , is available from the body of prior investigations of reactions 1 and -1 (in the case of the latter reaction because the thermochemistry of reactions 1, -1, i.e., the heat of formation of iso-C₃H₇, is now accurately known^{16,21}). The older literature on the kinetics of reactions 1, -1 has been reviewed by Tsang, who recommended an expression for k_1^∞ .¹⁶ In his evaluation, an incorrect expression for k_{-1}^∞ was used, resulting in an error of ≈ 1 kcal mol⁻¹ in a derived heat of formation of the isopropyl radical. This in turn created an error in the recommended expression for k_1^∞ . A new expression for k_1^∞ is presented here in the section dealing with the MSC/RRKM treatment of the data.

II. Experimental Section

(A) Apparatus and Procedure. Isopropyl radicals were produced in a heated flow reactor by pulsed laser photolysis of 2,4-dimethyl-3-pentanone diluted in an inert carrier gas (helium, argon, or nitrogen):



The subsequent decay of the iso-C₃H₇ radicals was monitored as a function of temperature and density using photoionization mass spectrometry. Radical concentrations were kept sufficiently low that the thermal decomposition process was essentially isolated for direct study. Details of the experimental apparatus²² and procedures^{23,24} have been published elsewhere and only those aspects of the procedures which are unique to the present study will be described in detail here.

Pulsed (≈ 5 Hz), unfocused 193-nm radiation from a Lambda Physik EMG 201 MSC excimer laser was directed along the axis of a heatable, uncoated quartz reactor (1.05-cm i.d.). Gas flowing through the tube at ≈ 4 m s⁻¹ contained the isopropyl radical precursor (2,4-dimethyl-3-pentanone) and an inert carrier gas (e.g., He) in large excess ($>99.9\%$). The flowing gas was completely replaced between laser pulses. Gas was sampled through a hole (0.043-cm diameter or 0.025-cm diameter) located at the end of a nozzle in the side of the reactor and formed into a beam by a conical skimmer before the gas entered the vacuum chamber containing the photoionization mass spectrometer. As the gas beam traversed the ion source, a portion was photoionized and mass selected. Temporal ion signal profiles were recorded on a multichannel scaler from a short time before each laser pulse up to 20 ms following the pulse. Data from 500 to 20 000 repetitions of the experiment were accumulated before the data were analyzed.

The initial iso-C₃H₇ concentrations were kept low (estimated to be typically less than 1×10^{11} molecule cm⁻³) so that reactions between photolysis products (including the C₃H₇ + C₃H₇ reaction) had negligible rates under the experimental conditions used in this study. Under these conditions the C₃H₇⁺ ion signal profiles were always exponential in shape and were fitted to an exponential function ($[\text{C}_3\text{H}_7^+]_t = [\text{C}_3\text{H}_7^+]_0 e^{-k't}$) by using a nonlinear least-squares procedure (e.g., see the insert in Figure 1). Below 650 K, the C₃H₇ decay constants (k') were independent of temperature for any given set of initial gas densities. This temperature-

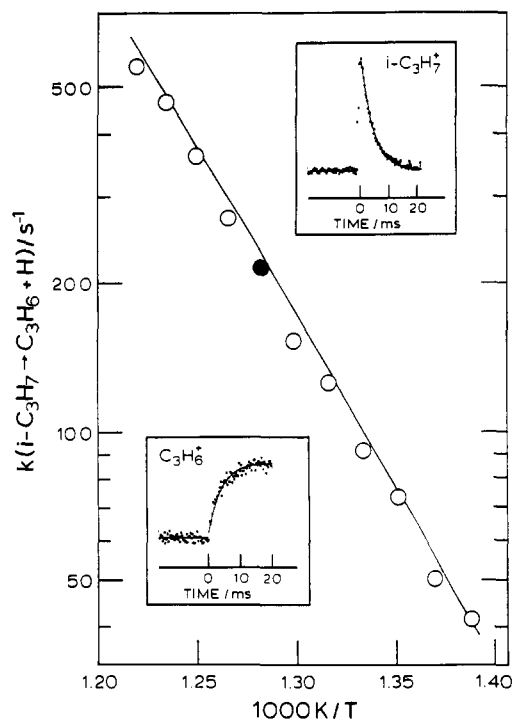


Figure 1. Plot of k_1 vs $1000/T$ obtained for a set of experiments with $[\text{He}] = 3.0 \times 10^{17}$ atoms cm⁻³ and $[(\text{iso-C}_3\text{H}_7)_2\text{CO}] = 9.4 \times 10^{12}$ molecules cm⁻³. Inserts are the iso-C₃H₇ and C₃H₆ signals recorded at 780 K (dark circle on plot). Line through the plotted rate constants are from the MSC/RRKM fit at this density. Lines through the plotted data points are from nonlinear least-squares fits of the data to single-exponential functions.

independent loss is attributed to heterogeneous processes:



Above 700 K the decay constant increased rapidly with rising temperature due to the increasing importance of the homogeneous thermal decomposition of the isopropyl radical. The C₃H₇ decay constants were analyzed assuming that the iso-C₃H₇ radicals were consumed only by the two elementary reactions 1 and 3. At low temperatures only the heterogeneous loss (reaction 3) is observed. Above 700 K the sum of the two loss processes is observed with the C₃H₇ exponential decay constant equal to $k_1 + k_3$ and, therefore, dependent only on temperature and the concentration of bath gas.

Before the sets of experiments designed to measure the C₃H₇ thermal decomposition rate were begun, a series of tests was performed to ensure that k' depended only on temperature and $[\text{M}]$. The isopropyl decay constants were found to be independent of precursor concentration (changed a factor of 9) and laser intensity (varied by a factor of 2). These results indicated that radical–radical reactions (such as C₃H₇ + C₃H₇) and radical–precursor reactions had negligible rates compared to that of the decomposition reaction. In addition, a small number of experiments were performed to measure the isopropyl decomposition using a different precursor and laser wavelength, the 248-nm photolysis of 2-bromopropane. The results were essentially identical to those obtained using the 2,4-dimethyl-3-pentanone although the heterogeneous loss rates were a factor of 2–3 higher and less reproducible. The results all support the conclusion that the mechanism (reactions 1 and 3) used to interpret the data is correct.

Sets of experiments were performed to determine k_1 as a function of temperature using different fixed gas densities. The C₃H₇ exponential decay constant, k' , was measured as a function of temperature (typically from 575 to 870 K) keeping the concentrations of all gases constant. Calculations of k_1 from measurements of k' require knowledge of k_3 above 650 K. While

k_3 (at the fixed total gas density) was directly determined below 650 K, it could not be measured above this temperature because of the additional loss of isopropyl by unimolecular decomposition. Below 650 K, k_3 was directly determined (because $k' = k_3$) and was found to be essentially temperature independent. Values of k_3 above 650 K needed for the data analysis were obtained by extrapolation assuming that k_3 retains this temperature independence up to the highest temperature of this investigation, 910 K. The determination of k_1 from one such set of experiments is shown in Figure 1.

To minimize possible errors in the determinations of k_1 caused by the assumed continued temperature independence of k_3 above 650 K, experiments to obtain k_1 were conducted at temperatures sufficiently high to assure that $k' > 3k_3$. It was this criterion that established the lowest temperature used to determine k_1 in each set of experiments. The highest temperature used at each total gas density was determined by the fact that decay constants above about 600 s^{-1} cannot be measured accurately.²⁵

Sets of experiments conducted at seven different helium densities ($(3\text{--}30) \times 10^{16} \text{ atoms cm}^{-3}$), four argon densities ($(3\text{--}9) \times 10^{16} \text{ molecules cm}^{-3}$) and three nitrogen densities ($(6\text{--}12) \times 10^{16} \text{ molecules cm}^{-3}$) provided sections of the unimolecular falloff curves (k_1 vs M) at different temperatures. Estimated uncertainties in the k_1 determinations range from $\pm 15\%$ in the middle of the temperature range to $\pm 25\%$ at the extreme temperatures used.

Photoionization in the mass spectrometer is provided by resonance lamps. A hydrogen lamp (10.2 eV) was used to photoionize $\text{C}_7\text{H}_{14}\text{O}$, $\text{C}_3\text{H}_7\text{Br}$, and C_3H_6 and a chlorine lamp (8.9–9.1 eV) to ionize $\text{iso-C}_3\text{H}_7$.

2,4-Dimethyl-3-pentanone (Aldrich, 98%) and 2-bromopropane (Aldrich, 99%) were purified by freeze–pump–thaw cycles before use. Helium (Matheson, 99.995%), argon (Matheson, 99.998%), and nitrogen (Matheson, 99.998%) were used as provided.

(B) Experimental Results. The $\text{iso-C}_3\text{H}_7$ thermal decomposition rate constant, k_1 , was determined as a function of inert gas density and temperature. Seventeen temperatures in the range 720–880 K were used in the experiments with helium. A 10-fold range of helium concentrations was covered ($(3\text{--}30) \times 10^{16} \text{ atoms cm}^{-3}$). Smaller ranges of temperatures and densities were encompassed in the experiments with argon ($T = 770\text{--}910 \text{ K}$; $[\text{Ar}] = (3\text{--}9) \times 10^{16} \text{ atoms cm}^{-3}$) and nitrogen ($T = 750\text{--}870 \text{ K}$; $[\text{N}_2] = (6\text{--}12) \times 10^{16} \text{ molecules cm}^{-3}$). The rate constant is in the falloff region under these experimental conditions.

The results of experiments used in the data analyses described below are plotted in Figures 2 and 3. In these plots, a reduced data set is shown, one which includes rate constants obtained at 14 of the 17 temperatures used, where the density dependence of reaction could be characterized. Typically, at the temperature extremes, only one or two densities could be employed.

Propene, the known product of the isopropyl thermal decomposition, was also detected and recorded. (Hydrogen atoms, the other product of the decomposition, cannot be detected using our photoionization system.) A small set of experiments was conducted to observe the temporal behavior of the propene. Its exponential growth constant was within $\pm 10\%$ of the isopropyl decay constant. (See the inset in Figure 1 for a typical example.) These experiments confirm the known radical decomposition mechanism and indicate that the products of the decomposition did not subsequently react in a manner that interfered with the essential isolation of the isopropyl decomposition process.

III. Data Analysis

The unimolecular rate constants obtained in the current investigation, $k_1(T, M)$, were analyzed using three procedures to model fall-off behavior. First, a MSC/RRKM analysis was used. Second, fits were made to the semiempirical analytical expression for the falloff in unimolecular rate constants introduced by Troe

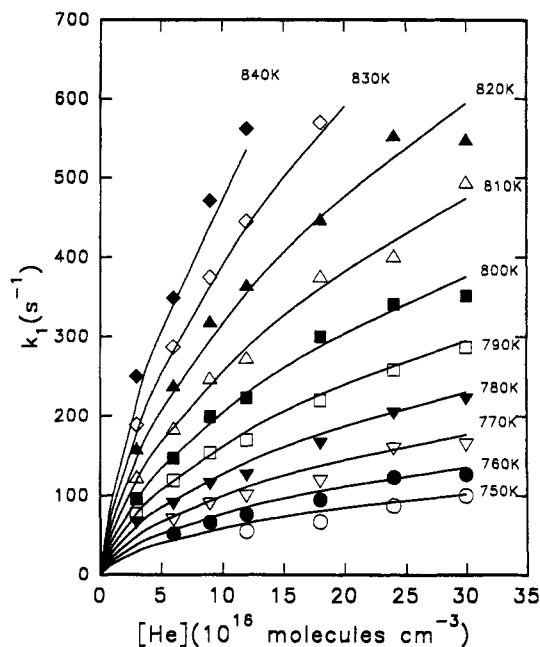


Figure 2. Plot of k_1 vs $[\text{He}]$. Lines through the experimental data are the MSC/RRKM fits.

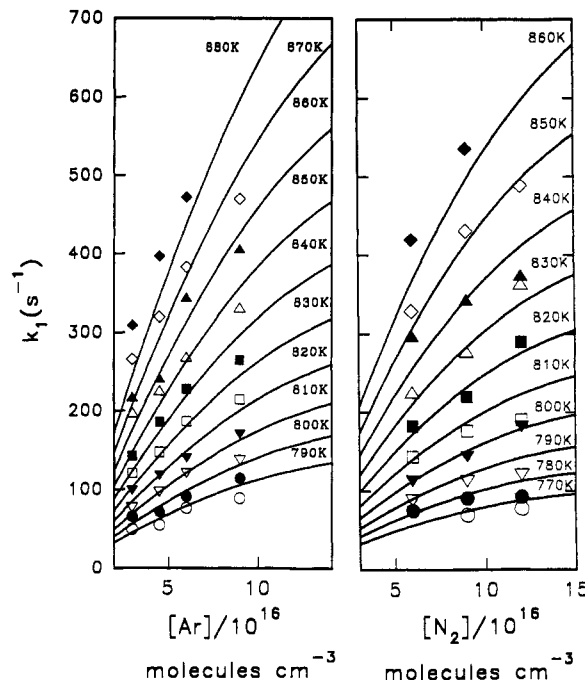


Figure 3. Plots of k_1 vs $[\text{Ar}]$ and $[\text{N}_2]$. Lines through the experimental data are the MSC/RRKM fits.

and co-workers. Finally, a master equation formulation was applied using an exponential-down model for the energy-dependent collision probabilities and $k(E)$ values obtained using inverse Laplace transformation of the high-pressure limit rate constant of the association reaction. All procedures provided some measure of $\langle \Delta E \rangle_{\text{down}}$, the average energy lost in deactivation collisions between the $\text{iso-C}_3\text{H}_7$ radical and the bath gases used. While values of this energy transfer parameter vary depending on the theoretical framework used to model weak collision effects, each provides a quantitative characterization of the energy transfer characteristics of reactions 1, –1 using a particular theoretical approach.

(A) Transition-State Model for Reactions 1, –1. In both the MSC/RRKM and the modified Lindemann–Hinshelwood analyses of the data a model for the transition state of reactions 1, –1 is required. One was created beginning with what is known about the transition state of the $\text{H} + \text{C}_2\text{H}_4 \rightleftharpoons \text{C}_2\text{H}_5$ reaction as

TABLE I: Thermodynamic Properties of the iso-C₃H₇ Radical Used in Present Analysis^a

temp, K	C _p ^o	S ^o	-(G _T ^o - H ₀ ^o)/T
200	13.94	62.83	51.36
298.16	16.84	68.89	56.18
300	16.90	69.00	56.26
400	20.71	74.38	60.12
500	24.47	79.41	63.48
600	27.84	84.18	66.53
700	30.80	88.69	69.37
800	33.39	92.98	72.06
900	35.66	97.05	74.61
1000	37.65	100.91	77.04

temp, K	H - H ₀	ΔH _T ^o	ΔG _T ^o	log K _p
200	2.294	22.812	30.665	-33.51
298.16	3.791	21.511 ^b	34.791	-25.50
300	3.822	21.486	34.873	-25.41
400	5.703	20.202	39.532	-21.60
500	7.963	19.067	44.498	-19.45
600	10.585	18.107	49.681	-18.10
700	13.522	17.315	55.012	-17.18
800	16.736	16.682	60.444	-16.51
900	20.195	16.194	65.947	-16.01
1000	23.864	15.828	71.498	-15.63

^a Standard pressure 1 bar. Units: for temperatures, K; for energies, cal mol⁻¹; for entropy, cal mol⁻¹ K⁻¹. Molecular properties from Table II. Hindered rotor contributions to thermodynamic functions were calculated from: Pitzer, K. S.; Gwinn, W. D. *J. Chem. Phys.* **1942**, *10*, 428. ^b Based on heat of formation at 298 K recommended in ref 21.

described in the experimental study of this reaction by Lightfoot and Pilling¹² and the theoretical study of Hase and Schlegel.²⁶ The properites of the transition state of reactions 1, -1, which bears a closer resemblance to C₃H₆ than to iso-C₃H₇, were initially obtained by modifying the molecular parameters for propene frequencies as follows:

(1) The frequencies assigned to the methyl group in propene were retained.

(2) Identical values were used for the low frequency C-H motions.

(3) The remaining frequencies were adjusted in the same ratio as the corresponding ethene/ethyl transition-state frequencies in the C₂H₅ → C₂H₄ + H reaction.

(4) A similar procedure was used to calculate the rotational constants for the transition state. Bond lengths and angles for the unchanged portion of the transition state were taken as the propene values. The remaining bond lengths and angles were based on the calculated geometry of the ethyl transition state.²⁶ The rotational constants were calculated to be 1.111, 0.276, and 0.254 cm⁻¹.

Treating the threshold energy of reaction 1 (E^o) as the only adjustable parameter of the transition state, a value was sought which provided the best agreement between calculated values of k₁^o (obtained using RRKM Theory) and experiment-based values of k₁^o which span the temperature range 177–673 K. The most accurate and direct determinations of k₁^o are those derived from reported values of k₋₁^o and the known thermochemistry of reactions 1, -1.^{16,21,27,28} The thermodynamic properties of iso-C₃H₇ used in the current study are given in Table I. The heat of formation at 298 K comes from a recent determination and data assessment of Seakins et al.²¹ The thermodynamic functions derived from partition functions (i.e., S^o, C_p^o, H - H^o) agree closely (within 0.8% between 300 and 1000 K, the temperature range of importance in this investigation) with those recently reported by Chen et al.²⁹ based on an ab initio study of the structure and internal motions of the iso-C₃H₇ radical. Priority was given to fitting k₁^o values obtained from the k₋₁ determinations at and below room temperature of Harris and Pitts,¹³ Watanabe et al.,³⁰ and Kurylo et al.¹⁴ since those measurements represent the high-pressure limit of reaction -1 and the agreement between these

TABLE II: Molecular and Transition-State Properties Used in the Analyses of the Data

Vibrational Frequencies (ν, cm ⁻¹)	
C ₃ H ₆ ³¹	3091, 3022, 2991, 2973, 2952, 2932, 1653, 1458, 1443, 1414, 1378, 1298, 1178, 1044, 990, 935, 919, 912, 575, 428
C ₃ H ₇ ³²⁻³⁴	3052, 2968(3), 2920, 2887, 2850, 1468, 1464, 1462, 1440, 1378, 1338, 1292, 1200, 1165, 1053, 922, 879, 748, 369, 364
C ₃ H ₇ [*]	3010, 2973(2), 2943, 2931, 2913, 1527, 1458, 1443, 1416, 1378, 1178, 1144, 1044, 934, 913, 895(2), 549, 425, 399, 369
Rotational Constants (A, B, C, cm ⁻¹)	
C ₃ H ₇	1.528, 0.274, 0.255 sym no. 2
C ₃ H ₇ [*]	1.111, 0.276, 0.254 sym no. 1
C ₃ H ₆	1.543, 0.290, 0.290 Symmetry number: 1
Methyl Torsional Rotational Constants ^a (cm ⁻¹), and Barrier Height (kcal mol ⁻¹) ^{27,29}	
C ₃ H ₆	7.09 sym no. 3 V ₀ 1.997
C ₃ H ₇	C ₃ H ₇ # = 6.66 sym no. 3 V ₀ 0.73
Critical Energy (E ^o): 35.85 kcal mol ⁻¹	
Lennard-Jones Parameters ³⁵	
C ₃ H ₇ =C ₃ H ₈	σ = 4.94 Å ε/k _b = 275 K
He	σ = 2.55 Å ε/k _b = 10 K
Ar	σ = 3.47 Å ε/k _b = 114 K
N ₂	σ = 3.74 Å ε/k _b = 82 K

^a In the MSC/RRKM calculation one external rotation (with the largest rotational constant) was treated as active degrees of freedom; the methyl torsion was treated as free motion.

studies is excellent. The value of E^o returned from this data fitting exercise was 35.9 kcal mol⁻¹.

All the transition-state properties used in the RRKM model are given in Table II along with the properties of C₃H₆ and iso-C₃H₇ used in the calculations described in section III.

The RRKM model and indicated thermochemistry for iso-C₃H₇ provide values of k₁^o and k₋₁^o in the temperature range 177–910 K which, when fitted to modified Arrhenius expression (k = AT_n exp(-E/T)), yield the following:

$$k_1^o = 6.51 \times 10^7 T^{1.83} \exp(-17793/T) \text{ s}^{-1} \quad (\text{I})$$

$$k_{-1}^o = 9.47 \times 10^{-15} T^{1.16} \times \exp(-440/T) \text{ cm}^3 \text{ molecule}^{-1} \text{ s}^{-1} \quad (\text{II})$$

The agreement between the experiment-based determinations of k₋₁^o and calculated values obtained using the transition-state model described above is excellent (see Figure 4). (k₋₁^o values obtained directly or indirectly (by conversion) from these studies are plotted instead of the corresponding k₁^o values in order to use a more expanded ordinate scale, one which can display small differences in rate constants). On Figure 4 we plotted k₋₁ instead of k₋₁^o in order to include k₋₁ determinations above room temperature which are close to the high-pressure limit. The deviation from the high pressure limit is estimated to be less than 40% at 473 K. Reported k₋₁ values are actually total addition rate constants and were corrected using Wagner and Zellner's expression for nonterminal H addition.¹⁵ This correction, which is negligible below room temperature, increases with increasing temperature and is 14% at the highest temperature (473 K) where total addition rate constants are available. Although the agreement between k₋₁^o obtained from the transition state model described above the k₋₁^o values obtained from the reported k₁^o is not very good one should keep in mind that these rate constants are functions of the equilibrium constant and, consequently, the heat of formation of the isopropyl radical. The agreement can be made perfect by lowering the heat of formation of the isopropyl radical by its reported error limit (0.4 kcal mol⁻¹).²¹

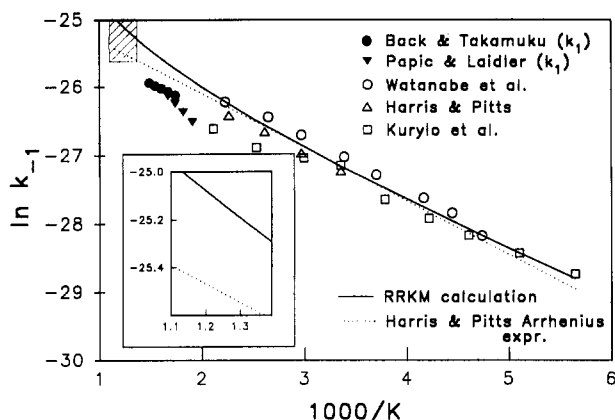


Figure 4. Plot of reported k_{-1}^{∞} vs $1000/T$. \circ , Watanabe et al.;³⁰ Δ , Harris and Pitts;¹³ \square , Kurylo et al.;¹⁴ \blacktriangledown , Papis and Laidler;¹⁴ \bullet , Back and Takamuku.¹⁰ The values of Papis and Laidler, Back and Takamuku were corrected for current values of the reference reaction and were taken from ref 36. Lines through data are from Harris and Pitts Arrhenius expression (dotted line), and from the RRKM model (solid line) described in section IIIA.

Included in Figure 4 with the corrected k_{-1} values are the RRKM rate constants k_{-1}^{∞} between 177 and 910 K and the Arrhenius expression for total H atom addition reported by Harris and Pitts for the temperature range 298–445 K, $k_{-1}^{\infty} = 2.21 \times 10^{-11} \exp(-1.56 \text{ kcal mol}^{-1}/RT) \text{ cm}^3 \text{ molecule}^{-1} \text{ s}^{-1}$.¹³ This Arrhenius expression was adopted by Tsang¹⁶ as the recommended expression for k_{-1}^{∞} . There is very good agreement between the RRKM rate constants for k_{-1}^{∞} and the corrected determinations of Harris and Pitts,¹³ Watanabe et al.,³⁰ and Kurylo et al.¹⁴ Agreement between RRKM rate constants and those obtained from the Arrhenius expression of Harris and Pitts is good throughout the temperature range of prior studies but obviously becomes poorer when extrapolations to higher and lower temperatures are considered. This increasing disagreement beyond the temperature extremes considered in the fitting exercise is expected and is caused by the temperature dependence of the Arrhenius parameters produced by the RRKM model (producing a small upward curvature of k_{-1}^{∞} and k_{-1} on Arrhenius plots). Deviations between the values of k_{-1}^{∞} from the RRKM model and extrapolated values using the Arrhenius expression of Harris and Pitts in the temperature range of the current study, 720–910 K (indicated by the shaded rectangle and by the insert in Figure 4), are as large as 65%. In sections IIIB and IIIC, we rely on extrapolations of k_{-1}^{∞} into the temperature range of our study provided by the RRKM model to interpret falloff behavior of reactions 1, -1.

In section IIID, an entirely different approach is used to interpret falloff behavior, one in which no transition-state model is required and the reaction threshold energy E° does not even appear explicitly. In this section, in which the ILT/ME technique is used, the reaction thermochemistry (ΔH°_0 of reaction 1, which of course, is itself uncertain to a degree) is floated instead of E° to help reproduce values of k_{-1} . In all the data treatments used below, $\langle \Delta E \rangle_{\text{down}}$ (or β_c) is an additional parameter used to reproduce the falloff behavior of k_{-1} . Since the reaction thermochemistry is treated as an adjustable parameter when the ILT/ME technique is used, the reported values of k_{-1}^{∞} and k_{-1} cannot arbitrarily be converted back and forth for convenience as is done in sections IIIB and IIIC where the reaction thermochemistry is presumed known.

In section IIID, the recommended Arrhenius expression for k_{-1}^{∞} , that reported by Harris and Pitts, is considered the basis of knowledge of the high-pressure-limit kinetic behavior of reactions 1, -1 at all temperatures, including the temperature range of our study, 720–910 K. At first glance, it appears that the data analyses in sections IIIB and IIIC use different high-pressure limit rate

constants for reactions 1, -1 from those used in section IIID in the analysis of weak collision effects. This difference is more apparent than real. The treatments in sections IIIB and IIIC rely heavily on the "known" reaction thermochemistry to obtain k_{-1}^{∞} values from reported determinations of k_{-1}^{∞} . A small change in the iso- C_3H_7 heat of formation (even within the reported uncertainty limits, $\pm 0.4 \text{ kcal mol}^{-1}$)²¹ would affect the conversion process and result in somewhat different recommended expressions for k_{-1}^{∞} and k_{-1} , from those given in eqs I and II.

It was considered of value to explore the analysis of weak collision effects in reactions 1, -1 using these very different approaches, ones which rely on different properties of this reaction. None is clearly preferable since each must accept the same uncertainty of the high-pressure-limiting behavior of reactions 1, -1 in the temperature range of our investigation.

(B) MSC/RRKM Analysis. The unimolecular rate constants of reaction 1 obtained in the current investigation were reproduced by computation using the unimolecular rate constant integral:

$$k_1(T, [M]) = \int_{E_0}^{\infty} k(E) P(E) dE / (1 + k(E)/\beta_c Z_{\text{coll}}^* [M]) \quad (\text{III})$$

where $k(E)$ is the microcanonical rate constant at energy E , $P(E)$ is the Boltzmann distribution function for active degrees of freedom, Z_{coll} is the Lennard-Jones collision frequency. The collision, efficiency, β_c , was used as an adjustable parameter to account for fall-off behavior of k_1 from the strong collision limit at each temperature used in our investigation. Each experimental falloff curve displayed in Figures 2 and 3 was fitted by using eq III, the transition-state model described in section IIIA, and by varying β_c . The calculated MSC/RRKM rate constants are superimposed as lines in the falloff plots shown in Figures 2 and 3. Priority was given to fitting the results obtained at the lower pressures where energy transfer effects are most manifest.

Each value of β_c thus obtained was converted to the more fundamental property, $\langle \Delta E \rangle_{\text{down}}$, using the expression provided by Troe³⁷ which is appropriate for a double exponential model for the energy-transfer transition probabilities:

$$\beta_c = (\langle \Delta E \rangle_{\text{down}} / (\langle \Delta E \rangle_{\text{down}} + F_E k_b T))^2 \quad (\text{IV})$$

where F_E is the energy dependence of the density of states and k_b is the Boltzmann constant. For the three bath gases used, the optimized values of the average step sizes down obtained from these collision efficiencies (eq IV) averaged over the temperature range of our study are as follows: 136 cm^{-1} (He), 130 cm^{-1} (Ar), and 129 cm^{-1} (N_2). An increase with temperature of $\langle \Delta E \rangle_{\text{down}}$ over the temperature range of our study was evidenced, but a detailed analysis of this trend is beyond the scope of the current study and will be dealt with later. We estimate the precision in the step sizes down to be $\pm 50 \text{ cm}^{-1}$.

Kurylo et al.¹⁴ report a small pressure dependence of the rate constant for addition of H atoms to propene, k_{-1} , at 298 K at pressures between 5–500 Torr of helium. We have carried out calculations of k_{-1} similar to those discussed above for k_1 . A very small step-size down, of the order of $20\text{--}40 \text{ cm}^{-1}$, is needed to account for any observable falloff behavior under these experimental conditions. This can be seen in Figure 5 where the experimental values of k_{-1} as well as calculated values using the three step sizes 20, 30, and 40 cm^{-1} are displayed. Kurylo et al. also obtained one value of k_{-1} at an elevated temperature, 473 K (in 50 Torr of He). Our calculations for this temperature require a step size in the range of $\approx 40 \text{ cm}^{-1}$.

Wagner and Zellner¹⁵ obtained k_{-1} values near 7 Torr of helium at temperatures between 195 and 390 K. When these values were fitted with the RRKM/MS model at two temperatures, 298 K (the same temperature as Kurylo et al.) and 390 K (the highest temperature of Wagner and Zellner study) $\langle \Delta E \rangle_{\text{down}}$ values of 13 cm^{-1} (298 K) and 34 cm^{-1} (390 K) were obtained.

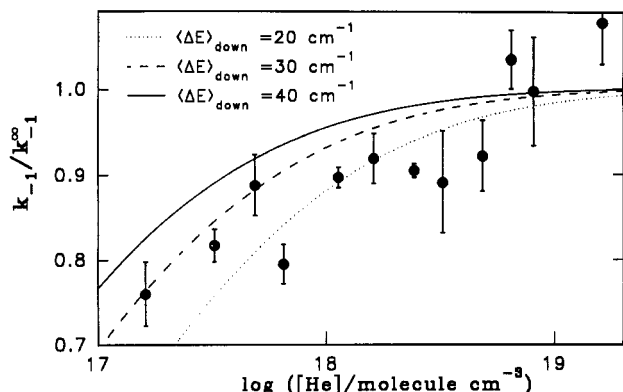


Figure 5. Plot of k_{-1}/k_{-1}^{∞} vs $\log [\text{He}]$ from data of Kurylo et al.¹⁴ Lines are calculated values using the MSC/RRKM model with different values of $\langle \Delta E \rangle_{\text{down}}$. Comparison indicates a value near 30 cm^{-1} is the most appropriate.

These values agree fairly well with the result derived from the experiments of Kurylo et al.

(C) **Modified Lindemann–Hinshelwood Analysis.** Troe and co-workers³⁸ have developed a semiempirical analytical expression for the falloff in the rate coefficient of a unimolecular reaction with pressure:

$$k_1/k_1^{\infty} = F_{\text{LH}} F^{\text{SC}} F^{\text{WC}} \quad (\text{V})$$

$$F_{\text{LH}} = \frac{k_1^{\circ} [\text{M}]/k_1^{\infty}}{1 + k_1^{\circ} [\text{M}]/k_1^{\infty}} \quad (\text{VI})$$

where k_1° and k_1^{∞} are the limiting low- and high-pressure rate coefficients and $[\text{M}]$ is the diluent density. F_{LH} is the Lindemann–Hinshelwood expression for k_1/k_1^{∞} , F^{SC} is a strong-collision term which corrects for the energy dependence of the microcanonical rate coefficients for dissociation, and F^{WC} corrects for the effects of weak collisions. F^{SC} depends primarily on S_{T} , the effective number of oscillators, and F^{WC} on S_{T} and on $\langle \Delta E \rangle_{\text{down}}$. Once k_1° and k_1^{∞} have been defined, S_{T} is the most critical of these parameters.

The model of the transition state needed to calculate S_{T} is given in section IIIA. S_{T} values in the range 6.83–7.60 were obtained as the temperature was increased from 750 to 830 K.

Fits of falloff behavior of k_1 in helium were initially made using a nonlinear least-squares procedure with k_1° and k_1^{∞} as variable parameters. Values of $\langle \Delta E \rangle_{\text{down}}$ between 100 and 250 cm^{-1} gave fits of comparable quality. Although the fits were good, the values of k_1^{∞} returned from the analysis gave an activation energy which is incompatible with the known thermochemistry. It is clear that the present data are so far from the high pressure limit that the unconstrained fits cannot give good estimates of k_1^{∞} . Accordingly, fits were performed with k_1^{∞} determined by the transition state model described in IIIA and only k_1° was floated. The optimum fits are shown in Figure 6.

Table III shows the optimum fitted values for k_1° determined with $\langle \Delta E \rangle_{\text{down}} = 200 \text{ cm}^{-1}$ for helium which are compared with values of k_1° calculated using the Troe factorization technique³⁹ with the same value of $\langle \Delta E \rangle_{\text{down}}$. The fitted data are within 50% of the calculated values over the temperature range 750–830 K. The fitted values of k_1° are comparatively insensitive to the value of $\langle \Delta E \rangle_{\text{down}}$ used in the fits, but are dependent on the value of k_1^{∞} used to constrain the fit. Decreasing k_1^{∞} by 50% at 790 K (corresponding to a simple Arrhenius extrapolation of k_1 from the experimental data on k_{-1}) increases the fitted values of k_1° from 5.6×10^{-15} to $1.11 \times 10^{-14} \text{ cm}^3 \text{ molecule}^{-1} \text{ s}^{-1}$.

The calculated value of k_1° is dependent on F^{WC} and hence $\langle \Delta E \rangle_{\text{down}}$. Unfortunately uncertainties in the correction factors used to calculate k_1° in the Troe factorization technique, and in

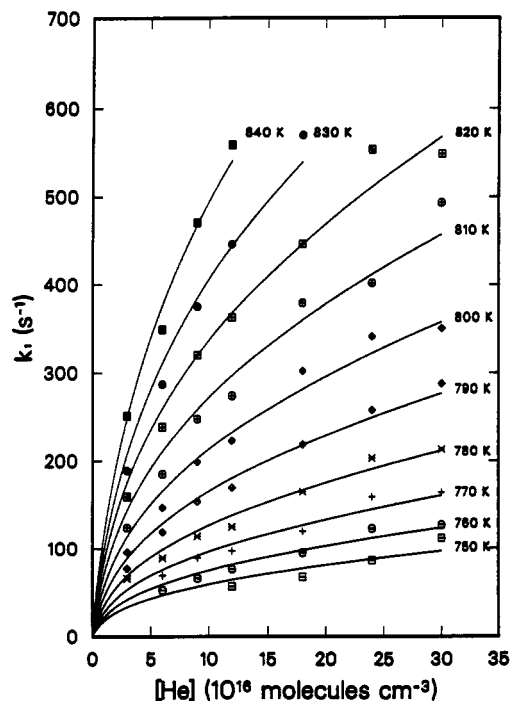


Figure 6. Plot of k_1 vs $[\text{He}]$. Lines through experimental data are fits from the modified Lindemann–Hinshelwood analysis.

TABLE III: Comparison of Experimental and Calculated Limiting Low-Pressure Rate Coefficients

T, K	$10^{15} k_1^{\circ}$ (calculated), ^a $\text{cm}^3 \text{ molecule}^{-1} \text{ s}^{-1}$	$10^{15} k_1^{\circ}$ (fitted), ^b $\text{cm}^3 \text{ molecule}^{-1} \text{ s}^{-1}$
750	3.7	2.2 ± 0.3
760	4.5	2.7 ± 0.2
770	5.6	3.4 ± 0.2
780	6.8	4.3 ± 0.2
790	8.1	5.6 ± 0.4
800	9.7	7.1 ± 0.6
810	11.9	8.9 ± 0.3
820	13.9	10.6 ± 0.7
830	16.6	13.1 ± 0.8

^a Based on the Troe factorization method.³⁹ ^b From fits to the experimental data using the Troe modified Lindemann–Hinshelwood method with $K_1^{\infty}(T)$ from section IIIA.

k_1^{∞} prevent the excellent agreement between the fitted and calculated values of k_1° being used to provide a quantitative estimate of $\langle \Delta E \rangle_{\text{down}}$.

(D) **Inverse Laplace Transform/Master Equation Analysis.** A more complete description of energy transfer and reaction in a unimolecular system is afforded by a discretized energy grained master equation formulation in which the energy of the isopropyl radical is divided into a contiguous set of grains, of width δ , each of which contains bundles of states to which a common averaged energy E_i is ascribed. For the present system the master equation takes the form:^{40–42}

$$dn_i(t)/dt = \omega \sum P_{ij} n_j(t) - (\omega + k_i) n_i(t) \quad (\text{VII})$$

where $n_i(t)$ is the time-dependent population density of grain i , ω is the collision frequency, P_{ij} is the probability transition for the transfer from grain j to grain i on collision, and k_i is the microcanonical (energy dependent) rate coefficient for unimolecular loss from grain i .

In the present case the decay at all but the shortest times is exponential and the rate coefficient for the decay, the unimolecular rate coefficient, can be determined by a standard eigenvalue analysis.⁴²

As has been discussed,⁴³ there is as yet no satisfactory universal expression for P_{ij} and so for the present the exponential down

model is used. For downward (deactivating) collisions:⁴⁴

$$P_{ij} = A_j \exp[-\alpha(E_j - E_i)] \quad j \geq i \quad (\text{VIII})$$

where

$$\alpha^{-1} = \langle \Delta E \rangle_{\text{down}} \quad (\text{IX})$$

A_j is an energy dependent normalization factor. P_{ij} must obey detailed balance allowing the calculation of the upward transition probabilities and hence the determination of A_j . The master equation is solved numerically. Standard techniques are described in ref 42. Our own approach, including the back-substitution procedure required to determine A_j , is given in ref 45.

Microcanonical rate coefficients can be obtained from temperature dependent data via the inverse Laplace transform (ILT) technique and its application to the recombination reaction of H atoms and propene (reaction -1). Such an approach is preferable to transformation of k_1^∞ in the present context, because the experimental addition rate coefficients are close to the high-pressure limit, are available over a reasonably wide range of temperatures and have only a weak dependence on temperature. The details of the techniques are given in ref 46; for the present case the pertinent equation is

$$k(E) \rho_A(E) = AC'(2/\sqrt{\pi}) \int_0^{E-E_a-\Delta H^\circ_0} \rho_{AB}(E')(E - (E' + E_a + \Delta H^\circ_0))^{1/2} dE' \quad (\text{X})$$

$$E \geq \Delta H^\circ_0 + E_a$$

for $k_1^\infty = A \exp(-E_a/RT)$. ΔH°_0 is the zero-point energy difference between reactants and products, ρ_A is the rovibrational density of states of the reactant (iso-C₃H₇), and ρ_{BC} is the rovibrational density of states of the products (propene and H). C' is given by

$$C' = \left[\frac{2\pi M_H M_{C_3H_6}}{h^2 M_{C_3H_7}} \right]^{3/2} \quad (\text{XI})$$

Equation X is written in terms of a continuous energy distribution. The microcanonical rate constants, k_i , incorporated in the master equation are the grain averages; their calculation from the continuous function $k(E)$ is discussed in ref 18.

Before eq X can be employed to determine $k(E)$, it is necessary to determine ρ_A and ρ_{BC} . The standard approach to such calculations is to invoke the rigid-rotor-harmonic oscillator (RRHO) approximation and to employ direct count techniques.⁴⁷ However, both C₃H₆ and iso-C₃H₇ have hindered internal rotors, with barrier heights, V_0 , which are comparable with kT (Table II). The large-amplitude motion is significantly coupled to the overall external rotation, so that the RRHO approximation is rather poor. This problem was examined in a recent analysis and satisfactory techniques developed to calculate ρ_A and ρ_{BC} ,⁴⁸ based on inverse Laplace transformation of the classical partition function for total rotation (internal and external). All densities of states calculations were performed using cell widths of 1 cm⁻¹, with a maximum energy of 20 000 cm⁻¹. The cells were combined into 50 cm⁻¹ grains for the master equation calculations.

The microcanonical rate constants, k_i , were calculated using eq X incorporating the Arrhenius parameters of Harris and Pitts¹³ (section IIIA). A number of checks was performed on the ILT procedure. The rovibrational partition functions for C₃H₆ and iso-C₃H₇ were calculated from the densities of states and compared with those calculated from standard analytic formulae.⁴⁸ For the temperature range 300–1000 K, the agreement was better than 98%. $k_{-1}^\infty(T)$ was calculated and combined with the equilibrium constant to determine $k_1^\infty(T)$, which agreed to better than 99% with those calculated from the Arrhenius parameters employed in the transformation.

TABLE IV: Gridpoint Values for 10⁻⁴χ²/s⁻² Close to the Surface Minimum

$\Delta H^\circ_0/\text{cm}^{-1}$ ($\Delta H^\circ_0/\text{kcal mol}^{-1}$)	$\langle \Delta E \rangle_{\text{down}}$		
	200	210	220
12 260 (35.05)	3.62	1.65	2.16
12 250 (35.02)	2.96	1.62	2.83
12 240 (35.00)	2.46	1.78	3.71

TABLE V: Values of χ² and Best-Fit $\langle \Delta E \rangle_{\text{down}}$ for ΔH°_0 Varied by ±1.2 kcal mol⁻¹ from the Optimal Value

$\Delta H^\circ_0/\text{cm}^{-1}$ ($\Delta H^\circ_0/\text{kcal mol}^{-1}$)	$\langle \Delta E \rangle_{\text{down}}/\text{cm}^{-1}$	10 ⁻⁴ χ ² /s ⁻²
12 668 (36.22)	380	7.50
11 832 (33.83)	130	10.78

The most facile approach to fitting the experimental data using the master equation model is to employ $\langle \Delta E \rangle_{\text{down}}$ as the single variable parameter. Such an approach would incorporate the data in Table II, together with ΔH°_0 , as fixed parameters. However it is of interest to investigate whether the temperature dependent falloff data allow a determination of ΔH°_0 .

A precise determination would be straightforward near the high pressure limit, since the dissociation rate constant is comparatively insensitive to $\langle \Delta E \rangle_{\text{down}}$. Under the present experimental conditions, however, which are well into the falloff region, the calculated values of k_1 are sensitive to both ΔH°_0 and $\langle \Delta E \rangle_{\text{down}}$ and there is a strong correlation between the best fit values of these two variable parameters. Nevertheless fits were investigated varying both parameters using minimum χ^2 :

$$\chi^2 = \sum_l (k_{\text{exp},l} - k_{\text{calc},l})^2 \quad (\text{XII})$$

as the criterion of best fit.

$k_{\text{exp},l}$ and $k_{\text{calc},l}$ are respectively the experimental and calculated rate constants at the conditions of temperature and pressure specified by the index l . The summation was taken over the whole data set for helium as the diluent gas. A simple grid search was employed to determine the position of the minimum; such an approach is preferred over a more sophisticated and computer-intensive gradient search approach because the region in which the minimum is likely to be located is defined through independent determinations of ΔH°_0 .

Table IV presents values of χ^2 for grid points in the vicinity of the well-defined minimum found at $\langle \Delta E \rangle_{\text{down}} = 210 \text{ cm}^{-1}$ and $\Delta H^\circ_0 = 12 250 \text{ cm}^{-1}$ (35.02 kcal mol⁻¹). Strong correlation between the two fitting parameters could lead to a flat valley on the χ^2 surface. The degree of correlation was investigated by varying ΔH°_0 by ±1.2 kcal mol⁻¹ and finding the surface minimum at these two extremes by varying $\langle \Delta E \rangle_{\text{down}}$. The results are shown in Table V, which demonstrates that these χ^2 minima are an order of magnitude larger than that given in Table IV. Clearly the surface minimum is well-defined and the experimental data can be used to obtain independent estimates of both $\langle \Delta E \rangle_{\text{down}}$ and ΔH°_0 . The calculated rate coefficients using the best fit values are compared with experiment in Figure 7.

The value of $\langle \Delta E \rangle_{\text{down}}$ is close to that determined by Hanning-Lee et al.¹⁸ for the similar C₂H₅ ⇌ H + C₂H₄ system at 800 K; Feng et al.¹⁷ obtained values of 229–282 cm⁻¹ in the temperature range 876–1094 K for the same system.

The best fit value for ΔH°_0 corresponds to $\Delta H^\circ_{f,298}$ (iso-C₃H₇) = 21.0 kcal mol⁻¹. The error limits are not well-defined, because of the limited analysis of the χ^2 surface but are likely to be less than ±1 kcal mol⁻¹. This value agrees well with the recent recommendation of Seakins et al.²¹ of 21.5 ± 0.4 kcal mol⁻¹.

IV. Discussion

The current investigation provides the first direct determinations of k_1 . Rate constants were obtained at 17 temperatures and

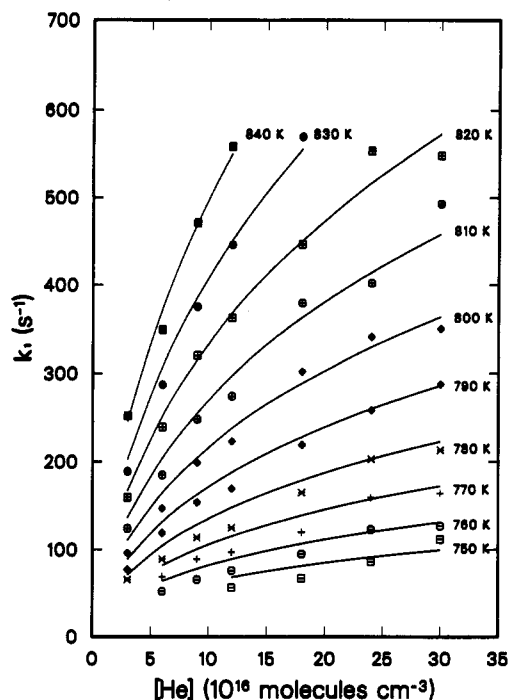


Figure 7. Plot of k_1 vs $[\text{He}]$. Lines through data are fits from the master equation analysis using the best-fit results of the grid search; $\Delta H^\circ_0 = 12\,250\text{ cm}^{-1}$ and $\langle \Delta E \rangle_{\text{down}} = 210\text{ cm}^{-1}$.

falloff behavior in k_1 was observed at 14 of these. The most significant problem in analyzing the data is that neither the high nor the low-pressure limit is approached under the experimental conditions, so that it is difficult to draw quantitative conclusions without additional information and/or a priori assumptions. Three approaches were employed.

The MSC/RRKM analysis requires the construction of a transition state model, based on literature values of $k_1^\circ(T)$ and $k_{-1}^\circ(T)$ and prior knowledge of the thermodynamic properties of iso-C₃H₇. The procedure allows a simple integral representation of $k_1([M], T)$ but is based on a modified strong collision approach.

The reaction rate distribution function for reaction 1, $k(E_R)\rho(E_R)\exp(-E_R/kT)$, peaks approximately 3500 cm⁻¹ above the threshold energy at 800 K (Figure 8), indicating that the master equation model, which explicitly recognizes the multistep nature of energy transfer, is more appropriate. Nevertheless, the estimates of $\langle \Delta E \rangle_{\text{down}}$ derived from the two approaches are broadly comparable.

The Troe modified Lindemann-Hinshelwood formulation is widely employed to fit experimental data and to provide an economical representation of the pressure and temperature dependence of the rate coefficient for incorporation in numerical simulations of complex reactions. The shape of the falloff curve depends primarily on k_1° , k_{-1}° , and S_T ; in the present analysis, k_1° and S_T were fixed and k_{-1}° was the major variable parameter. $\langle \Delta E \rangle_{\text{down}}$ was varied, but its effects are of only secondary importance. k_{-1}° implicitly contains information on $\langle \Delta E \rangle_{\text{down}}$ but this information can be revealed only if the strong collision limiting rate coefficient is calculated from first principles; such a procedure is not a satisfactory means of determining $\langle \Delta E \rangle_{\text{down}}$ precisely.

Inverse Laplace transformation of the addition rate coefficient, coupled with the master equation approach permits the analysis of the data with a minimum of assumptions. In effect the process of constructing a transition state model, which is adjusted by reference to $k_{-1}^\circ(T)$, is by-passed and the microcanonical rate constants for dissociation are related directly to the canonical rate coefficient via the molecular properties of the reactants and products. The energy dependence of $k(E_R)$ is a sensitive function of the temperature dependence of k_{-1}° . A wide range of

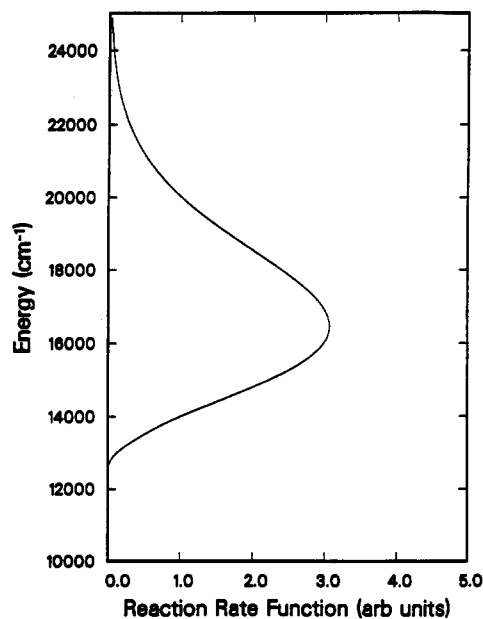


Figure 8. Plot of energy in iso-C₃H₇ active degrees of freedom vs. reaction rate function, $(k(E_R)\rho(E_R)\exp(-E_R/kT))$. The function has a maximum at iso-C₃H₇ energies approximately 3500 cm⁻¹ above the reaction threshold.

experimental temperatures, strictly an infinite range, should be employed for precise definition of $k(E_R)$. We have demonstrated, however, through model calculations, that a satisfactory form for $k(E_R)$ can be generated even if k_{-1}° has been measured over only a modest range of temperatures.⁴⁹ The use of association rate coefficients has considerable advantages over the transformation of dissociation coefficients because the temperature dependencies of the former are weak and are not swamped by the contribution of the dissociation energy.

The major problem with the inverse Laplace transformation approach is that, while rotational energy is included in the state counting procedures, rotational energy states cannot be treated explicitly, i.e., $k(E, J)$ cannot be calculated. To some extent this problem is ameliorated, because differential relaxation of vibrational and rotational energies is difficult to incorporate into a master equation model and no generally satisfactory method of solution exists. Nevertheless the interplay between these two types of energy transfer may be significant in determining the average values of $\langle \Delta E \rangle_{\text{down}}$ determined by the technique. A related aspect of this problem, namely the effect of changing the number of active rotors, has been discussed previously for the H + C₂H₄ system.¹⁷

All three methods of data analysis provide similar estimates of $\langle \Delta E \rangle_{\text{down}}$ for He, in the range 136–210 cm⁻¹ at temperatures near 800 K. The MSC/RRKM analysis gives values close to those found, using a similar approach, for the neopentyl radical at slightly lower temperatures (560–650 K) and the general trend in collision efficiencies is similar for the two radicals.²⁴ The ILT/ME approach gives a $\langle \Delta E \rangle_{\text{down}}$ value very close to those determined for C₂H₅ (190–200 cm⁻¹ at 800 K).¹⁸

The analysis of the C₂H₅ ⇌ H + C₂H₄ system demonstrated a strong dependence of $\langle \Delta E \rangle_{\text{down}}$ on T , increasing from 30–40 cm⁻¹ at 300 K to 280 cm⁻¹ at 1100 K. The MSC/RRKM analysis of the room-temperature data of Kurylo et al.¹⁴ and Wagner and Zellner¹⁵ for H + C₃H₆ ($\langle \Delta E \rangle_{\text{down}} = 20\text{--}30\text{ cm}^{-1}$) suggests that $\langle \Delta E \rangle_{\text{down}}$ also depends on temperature for this system. It should be recognized, however, that k_{-1} is close to its high-pressure limit under the conditions of this study as well as in all prior investigations of reaction -1.^{13-15,30} Hence only a small uncertainty in the limiting high pressure rate coefficient leads to a very large error in the step-size down parameter when fitting published falloff behavior. Therefore it is difficult to extract accurate

information on the temperature dependence of $\langle \Delta E \rangle_{\text{down}}$ by combining information from the current study with that obtained from prior investigations. There is clearly a need for measurements of k_{-1} deeper in the falloff region either at higher temperatures or at lower pressures (below 0.5 Torr) than have been used before in order to establish the temperature dependence of $\langle \Delta E \rangle_{\text{down}}$ more precisely.

Although the reaction is well into the falloff region under the experimental conditions, the ILT/ME analysis demonstrates that a reliable estimate of ΔH°_0 can be obtained. In effect, the experimental $k_1([M], T)$ values have been combined with the literature values of k_{-1} and the molecular parameters of reactants and products to determine ΔH°_0 . Even though there is some correlation between $\langle \Delta E \rangle_{\text{down}}$ and ΔH°_0 , the minimum is sufficiently well-defined for an estimate of ΔH°_0 to be obtained from the analysis.

Acknowledgment. We thank the Office of Basic Energy Sciences, Office of Energy Research, U.S. Department of Energy under Grant No. DE/FG05-89ER14015, the Science and Engineering Council, U.K., ICI plc and NATO (Research Grant 0518487) for supporting this research. This collaboration was made possible in part through NATO Research Grant 0518/87 and this contribution is also gratefully acknowledged.

Supplementary Material Available: Table S1, listing the conditions and results of all experiments to measure k_1 , the unimolecular rate constant for the thermal decomposition of the iso-C₃H₇ radical (10 pages). Ordering information is given on any current masthead page.

References and Notes

- (1) Hucknall, D. J. *Chemistry of Hydrocarbon Combustion*; Chapman and Hall: New York, 1985.
- (2) Kerr, J. A.; Parsonage, M. J. *Evaluated Kinetic Data on Gas Phase Addition Reactions*; Butterworth: London, 1972.
- (3) McMillen, D. F.; Golden, D. M. *Annu. Rev. Phys. Chem.* **1982**, *33*, 493.
- (4) Papic, M. M.; Laidler, K. J. *Can. J. Chem.* **1971**, *49*, 549.
- (5) Camilleri, P.; Marshall, R. M.; Purnell, H. J. *Chem. Soc., Faraday Trans. 1* **1975**, *71*, 1491.
- (6) Pratt, G.; Rodgers, D. J. *Chem. Soc., Faraday Trans. 1* **1979**, *75*, 1089.
- (7) Pacey, P. D.; Wimalasena, J. H. J. *Phys. Chem.* **1984**, *88*, 5657.
- (8) Trenwith, A. B. J. *Chem. Soc., Faraday Trans. 2* **1986**, *82*, 457.
- (9) Canosa, C. E.; Marshall, R. M. *Int. J. Chem. Kinet.* **1981**, *13*, 303.
- (10) Back, R. A.; Takamuku, S. J. *Am. Chem. Soc.* **1964**, *86*, 2558.
- (11) Payne, W. A.; Stief, L. J. *J. Chem. Phys.* **1976**, *64*, 1150.
- (12) Lightfoot, P. D.; Pilling, M. J. *J. Phys. Chem.* **1987**, *91*, 3373.

- (13) Harris, G. W.; Pitts, J. N., Jr. *J. Chem. Phys.* **1982**, *77*, 3994.
- (14) Kurylo, M. J.; Peterson, N. C.; Braun, W. J. *Chem. Phys.* **1971**, *54*, 4662.
- (15) Wagner, H. Gg.; Zellner, R. *Ber. Bunsen-Ges. Phys. Chem.* **1972**, *76*, 440.
- (16) Tsang, W. J. *Am. Chem. Soc.* **1985**, *107*, 2872.
- (17) Feng, Y.; Niiranen, J. T.; Bencsura, A.; Knyazev, V. D.; Gutman, D.; Tsang, W. J. *Phys. Chem.*, submitted for publication.
- (18) Hanning-Lee, M. A.; Green, N. J. B.; Pilling, M. J.; Robertson, S. H. *J. Phys. Chem.*, submitted for publication.
- (19) Bencsura, A.; Knyazev, V. D.; Slagle, I. R.; Gutman, D.; Tsang, W. *Ber. Bunsen-Ges. Phys. Chem.*, accepted for publication.
- (20) Tsang, W. *Combustion Flame* **1989**, *78*, 71.
- (21) Seakins, P. W.; Pilling, M. J.; Niiranen, J. T.; Gutman, D.; Krasnoperov, L. N. *J. Phys. Chem.* **1992**, *96*, 9847.
- (22) Slagle, I. R.; Gutman, D. *J. Am. Chem. Soc.* **1985**, *107*, 5342.
- (23) Timonen, R. S.; Ratajczak, E.; Gutman, D.; Wagner, A. F. *J. Phys. Chem.* **1987**, *91*, 5325.
- (24) Slagle, I. R.; Batt, L.; Gmurczyk, G. W.; Gutman, D.; Tsang, W. J. *Phys. Chem.* **1991**, *95*, 7732.
- (25) Moore, S. B.; Carr, R. W. *Int. J. Mass Spectrom. Ion Phys.* **1977**, *24*, 161.
- (26) Hase, W. L.; Schlegel, H. B. *J. Phys. Chem.* **1982**, *86*, 3901.
- (27) Chao, J.; Zwolinski, B. J. *J. Phys. Chem. Ref. Data* **1975**, *4*, 251.
- (28) Chase, M. W. Jr.; Davies, C. A.; Downey, J. R. Jr.; Frurip, D. J.; McDonald, R. A.; Syverud, A. N. *J. Phys. Chem. Ref. Data* **1985**, *14*, 1.
- (29) Chen, Y.; Rauk, A.; Tschuikow-Roux, E. *J. Phys. Chem.* **1990**, *94*, 2775.
- (30) Watanabe, T.; Kyogoku, T.; Tsumashima, S.; Sato, S.; Nagase, S. *Bull. Chem. Soc. Jpn.* **1982**, *55*, 3720.
- (31) Silvi, B.; Labarbe, P.; Perchard, J. P. *Spectrochim. Acta* **1973**, *29A*, 263.
- (32) Gayles, J. N. Jr.; King, W. T. *Spectrochim. Acta* **1965**, *21*, 543.
- (33) Chettur, G.; Snelson, A. *J. Phys. Chem.* **1987**, *91*, 913.
- (34) Pacansky, J.; Coufal, H. *J. Chem. Phys.* **1980**, *72*, 3298.
- (35) Hippler, H.; Troe, J.; Wendelken, H. J. *J. Chem. Phys.* **1983**, *78*, 6709.
- (36) Tsang, W. J. *Phys. Chem. Ref. Data* **1988**, *17*, 887.
- (37) Troe, J. *J. Chem. Phys.* **1977**, *66*, 4715.
- (38) Troe, J. *Ber. Bunsen-Ges. Phys. Chem.* **1974**, *78*, 478.
- (39) Gilbert, R. G.; Luther, K.; Troe, J. *Ber. Bunsen-Ges. Phys. Chem.* **1983**, *87*, 169.
- (40) Oppenheim, I.; Shuler, K. E.; Weiss, G. H. *Stochastic Processes in Chemical Physics: The Master Equation*; M.I.T. Press: Cambridge, MA, 1977.
- (41) Green, N. J. B.; Marchant, P. J.; Perona, M. J.; Pilling, M. J.; Robertson, S. H. *J. Chem. Phys.*, submitted for publication.
- (42) Gilbert, R. G.; Smith, S. C. *Theory of Unimolecular and Recombination Reactions*; Blackwell: Oxford, 1990.
- (43) Oref, I.; Tardy, D. C. *Chem. Rev.* **1990**, *90*, 1407 and references therein.
- (44) Penner, A. P.; Forst, W. *J. Chem. Phys.* **1977**, *67*, 5296.
- (45) Green, N. J. B.; Pilling, M. J.; Robertson, S. H., to be published.
- (46) Davies, J. W.; Green, N. J. B.; Pilling, M. J. *J. Chem. Phys. Lett.* **1986**, *126*, 373.
- (47) Beyer, T.; Swinehart, D. F. *Commun. Assoc. Comp. Machin.* **1973**, *16*, 379.
- (48) Stein, S. E.; Rabinovitch, B. S. *J. Chem. Phys.* **1973**, *58*, 2438.
- (49) Robertson, S. H.; Wardlaw, D. *Chem. Phys. Lett.*, in press.
- (49) Davies, J. W.; Green, N. J. B.; Pilling, M. J., to be published.